A High-efficiency Modular Switched-Capacitor Converter with Continuously Variable Conversion Ratio

Mohammed Khorshed Alam and Faisal H. Khan
Power Engineering and Automation Research Lab (PEARL)
Dept. of Electrical and Computer Engineering,
Univ. of Utah, Salt Lake City, USA
Email: khorshed.alam@utah.edu

***Abstract*— The multilevel modular capacitor clamped converter (MMCCC) topology overcomes the difficulties of the multilevel switched capacitor (SC) based dc-to-dc converters in high conversion ratio applications. MMCCC is completely modular and has many other advantageous features. Like most other SC converters, MMCCC suffers from limited voltage regulation. The conversion ratio of an ideal MMCCC converter in step-up mode is an integer, and this integer conversion ratio depends on the number of active modules. The maximum conversion ratio in step-up configuration for a k-module MMCCC is (k+1). It has already been shown in literature that different integer CRs can be achieved by changing the number of active modules of an MMCCC. Achieving voltage regulation by lowering the operating frequency is another well known technique for switched capacitor converters. However, the output voltage ripple increases in inverse proportion of the frequency. In this paper, a new switching scheme is proposed for MMCCC to achieve continuously variable CRs. The proposed switching scheme requires introducing a small inductor in each module of the MMCCC without altering the modular structure of the converter. This additional inductor can be realized using the stray inductance distributed in the circuit or small external inductors. It has been shown that continuous CR variation with lower output ripple can be achieved without lowering the operating frequency of the converter. This proposed method introduces another degree of freedom in order to achieve variable CR using MMCCC. Simulation results and experimental results obtained from an MMCCC prototype have been used to validate the new control scheme.**

I. INTRODUCTION

Switched capacitor (SC) converters have many advantageous features compared to inductor based dc-to-dc converters. SC converters can be designed to be light-weight, compact, highly efficient, and are well suited for monolithic integration [1]-[3]. The multilevel modular capacitor clamped converter (MMCCC) topology is completely modular and has many advantageous features. MMCCC is bi-directional, scalable to any number of modules, can achieve high conversion ratio (CR). The maximum voltage stress on the switches does not increase with increased number of modules. MMCCC can be used for multiple load source integration and possesses a high utilization factor. Similar to other switched-capacitor converters, MMCCC suffers from limited voltage regulation. In step up mode, the achievable conversion ratios are only integers. In step down mode the conversion ratios of an ideal MMCCC is the reciprocal of integer numbers [4]-[12]. A quasi-resonant strategy for the MMCCC (ZCS-MMCCC) without any additional components to achieve ZCS for all the switches is proposed in [13][14]. This ZCS-MMCCC structure requires a resonant inductor in each modules of the MMCCC. This inductance is realized by stray inductances distributed in the circuit. The ZCS-MMCCC reduces the switching losses of the converter. Therefore, the efficiency of the converter is increased. However, the circuit still suffers from limited voltage regulation.

In this paper a new switching scheme has been proposed for MMCCC in order to achieve fractional variable CRs, and the CR can be continuously varied during the normal operation of the converter. This switching scheme requires a small inductor in each module that can be realized using small an air core inductor or commercially available ferrite core inductors. Schematic diagram of a module of MMCCC with an additional inductor is shown in Fig. 1(a), and the complementary two phase switching pattern used in MMCCC is shown in Fig. 1(b). The switching pattern proposed in this paper is generated by

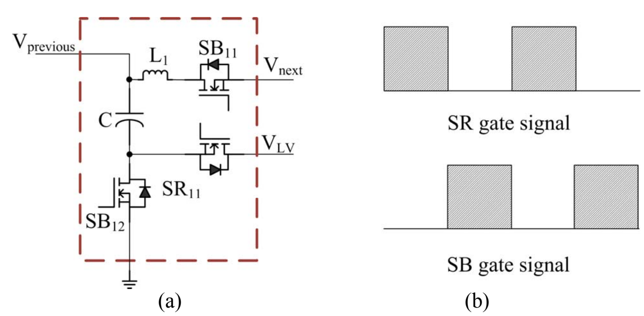

Fig. 1. (a) Schematic of a module of MMCCC with an additional inductor. (b) The complementary switching pattern used in MMCCC.

978-1-4244- 9373-9/12/$26.00 ©2012 IEEE

comparing a variable amplitude square wave with a fixed amplitude triangular wave. For an ideal MMCCC with k-modules in step-up mode, the maximum output voltage is (k+1) times the low side voltage. It has been observed that the CR can be varied from (k+1) to k by varying the amplitude of the square wave. Moreover, MMCCC can achieve variable integer CRs by changing the number of active modules. Therefore, using the proposed technique and changing the number of active modules as discussed in [7], it is possible to achieve a wide range of continuously varying CR using MMCCC.

This paper is organized in the following manner: The basic operation of the MMCCC topology is presented in section II. The proposed switching scheme is discussed in section III. The simulation and experimental results are presented in section IV and V, respectively. Finally, the paper is briefly summarized in section VI.

II. MMCCC TOPOLOGY

MMCCC is a modular SC converter. Each module is consists of one capacitor and three switches. The proposed switching scheme requires an additional inductor in each module as shown in Fig 1. The structure of the MMCCC is such that an inductor can be placed in each module without any need for additional snubber circuit. This feature is important in order to protect the switches from high voltage stress resulting from the residual current of the inductor during switching transient. A k-module MMCCC discussed here requires (3k+1) transistors, (k+1) capacitors and k number of inductors. The schematic diagram of a 5-module MMCCC with an external inductor in each module is shown in Fig. 2. The equivalent circuits of a 5-module MMCCC during two operating states are shown in Fig. 3, where V_{LV} is the low-side input voltage in step up mode. The maximum voltage stress of the switches SB_{i2} and SR_{i2} (i=1, 2,…,6) is two times the low-side input voltage regardless of the number of assembled modules. The maximum voltage stress on capacitor C_1 is V_{LV}. The

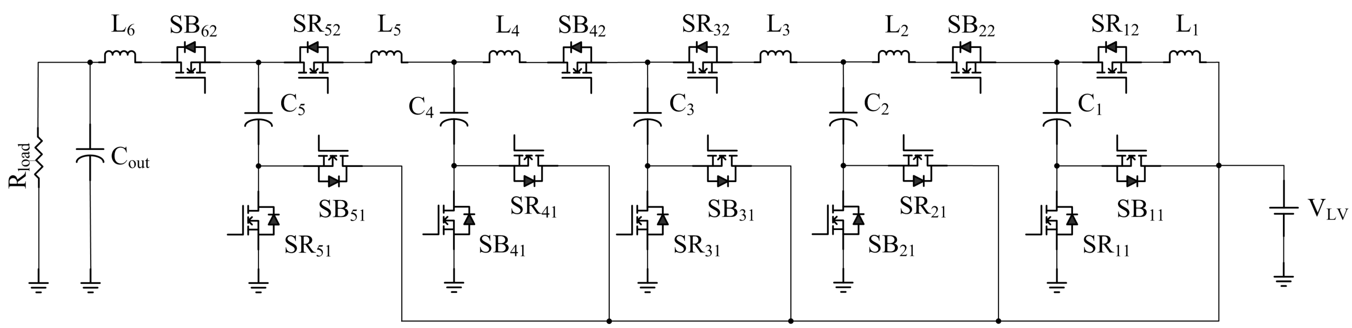

Fig. 2. Schematic of a 5-module MMCCC with an additional inductor in each module.

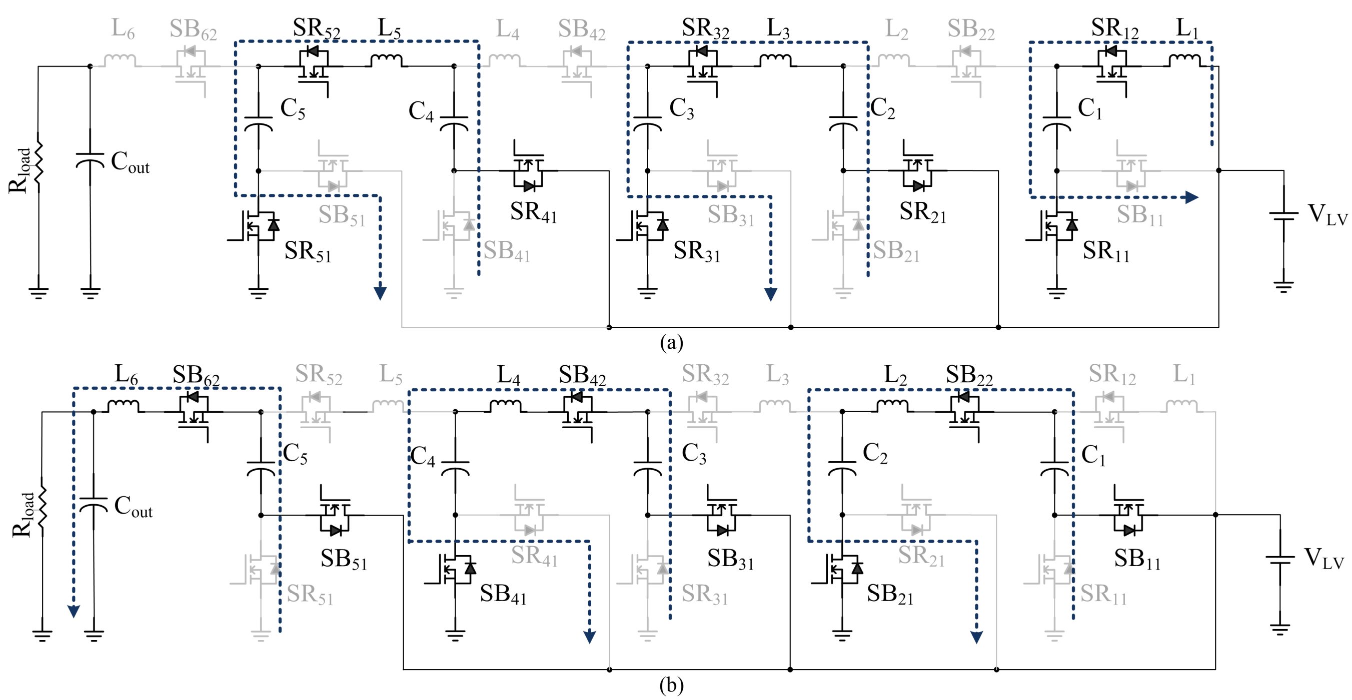

Fig. 3. MMCCC during two different states. (a) State 1: SR switches are ON and SB switches are OFF. (b) State 2: SB switches are ON and SR switches are OFF. The blue dashed line shows the residual current path during the phase transition.

maximum voltage stress on other capacitor increases by V_{LV} in each consecutive modules. For example, the maximum voltage stress on the capacitor C_2 is two time of V_{LV}.

Depending on the phase of the gate signal clock, all the switches in the MMCCC circuit can be divided into two groups: SR and SB. During the first phase of the clock signal, SR transistors are activated. SB transistors are activated during the second phase of the clock. During transition from one switching phase to another switching phase, there must be some current path for the residual current flow of the inductors. In Fig. 3, the current paths for the residual inductor current are shown using blue dashed lines.

The SB_{i1} and SR_{i1} (i=1, 2,… , 5) switch pair of each module can be driven using a bootstrap half bridge driver. Similarly the switch pair SR_{i2} (i=1, 3, 5) and SB_{i2} (i=2, 4, 6) of adjacent modules can be driven using another bootstrap half bridge driver. Therefore, a 5-module MMCCC can be driven using eight bootstrap half bridge drivers. The inductors are placed in the circuit by considering the requirement of the gate driver circuit.

III. PROPOSED SWITCHING SCHEME

The proposed switching pattern is generated by comparing a square wave with a triangular wave. A variation in CR can be obtained by varying the amplitude of the square wave. Similar to SPWM, two modulation indexes can be introduced here: amplitude modulation index (m_a) and frequency modulation index (m_f). Amplitude modulation index may be defined as in equation (1).

$$m_a = \frac{\hat{v}_{sqr}}{\hat{v}_{tri}} \qquad (1)$$

Where, $\hat{v}_{sqr}$ is the peak-to-peak amplitude of the square wave signal and $\hat{v}_{tri}$ is the amplitude of the triangular wave. Here m_a can be varied from 0 to 1.

Similarly, the frequency modulation index may be defined as in equation (2).

$$m_f = \frac{f_{sqr}}{f_{tri}} \qquad (2)$$

Where, f_{sqr} and f_{tri} are the frequencies of the square wave signal and the triangular wave signal respectively. In Fig. 4, the detail of the construction of gate signals are shown for m_a=0.6 and 0.3 for a fixed m_f equal to 5.

It should be noted that the resulting clock signals consists of two different segments depending on the values of m_a and m_f. One segment consists of pulses with fixed pulse width equal to $1/f_{sqr}$. It should be noted that a pulse having smaller width might occur at the boundaries of this section as shown in Fig. 4(e) and Fig. 4(f). Therefore, the MMCCC is switched at a constant frequency equal to f_{sqr} in this segment except at the boundaries. During the other segment, the switching signal has a fixed value. The clock signal is either 1(Fig. 4(b) and

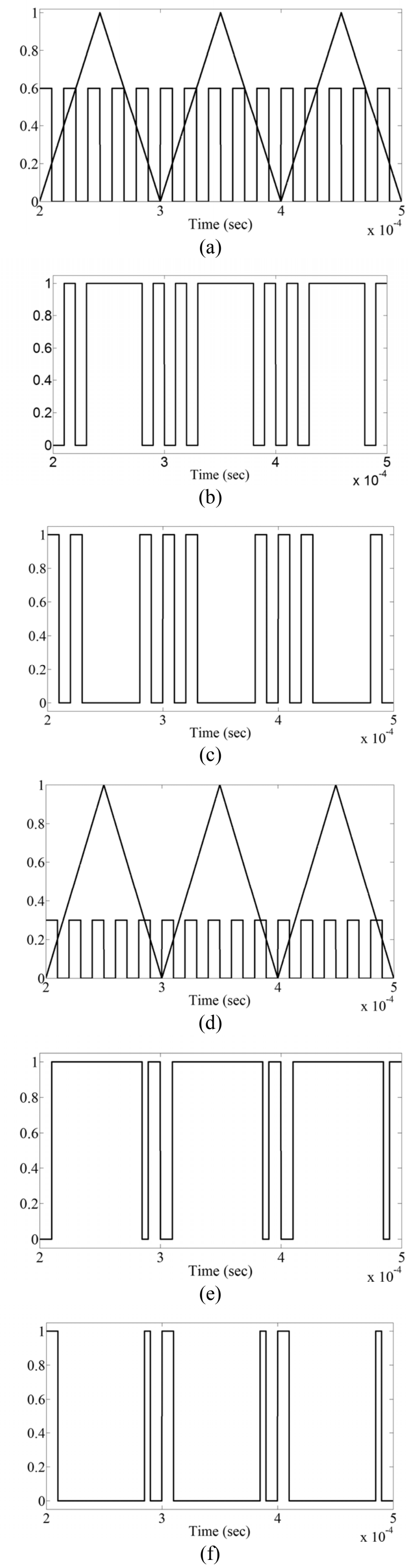

Fig. 4. For (a)-(c), m_a=0.6 and for (d)-(f), m_a=0.3. Square wave of different amplitudes with fixed amplitude triangular wave are shown in (a) and (d). Complementary gate signals for m_a=0.6 are shown in (b)-(c). Complementary gate signals for m_a=0.3 are shown in (e)-(f).

Fig. 4(e)) or 0 (Fig. 4(c) and Fig. 4(f)) for longer time span depending on the values of m_a.

IV. SIMULATION RESULTS

In order to verify the proposed control schemes, an MMCCC having five modules was simulated in PSIM. A capacitor of 4.7μF with 0.05 Ω equivalent series resistance (ESR) was used for each module. The converter was loaded with a fixed 150 Ω load. During the simulation, the R_{DS} of all the MOSFETs was assumed to be equal to 10 mΩ. The inductor in each module was set to 1 μH inductor with a dc equivalent resistance of 0.01 Ω. The low side input voltage was maintained at 10 V. The switching frequency of the triangular wave and the square wave were fixed at 10 kHz and 50 kHz respectively. The output voltage was observed for different values of amplitude modulation index (m_a). The simulation was performed for 3, 4 and 5- modules. At no load the maximum CR is 6, and the maximum CR depends on the load resistance. Maximum CR decreases with decrease in load resistance. For obvious reasons, the output voltage ripple increases with decrease in load resistance. Maximum CR is observed around the maximum value of amplitude modulation index (m_a=1.0). The CR decreases with the decrease in m_a. In order to achieve a continuously variable CR, it is required to achieve the dynamic range of CR variation equal to 1 for a fixed number of active modules. The variation of CR vs. m_a is shown in Fig. 5. It should be noted that, the change of CR vs. m_a is not linear. The CR drops more rapidly as m_a varies from 1 to 0. Inserting an additional inductor in each module decreases the peak input current while achieving variable CR. Moreover, the dv/dt stress on each capacitor is also reduced.

V. EXPERIMENTAL RESULTS

In order to verify the simulation results, a 5-module reconfigurable MMCCC prototype was built and tested in the laboratory setup. The prototype was built in a way such that it can be configured into a 3 or 4-module MMCCC by bypassing one or two modules. All the switches are implemented using a 100V 43 A MOSFET (IRFI4410ZPBF) in parallel with a 100V 30A schottky diode (STPS30SM100S). The schottky diode helps to carry the residual currents of the inductors during the

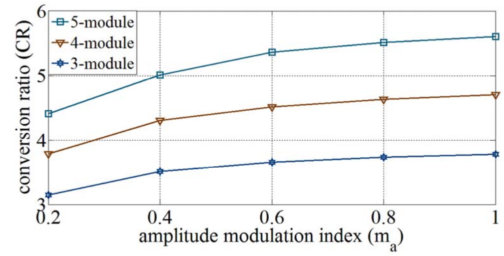

Fig. 5. Simulation results: conversion ratio vs. amplitude modulation index (m_a).

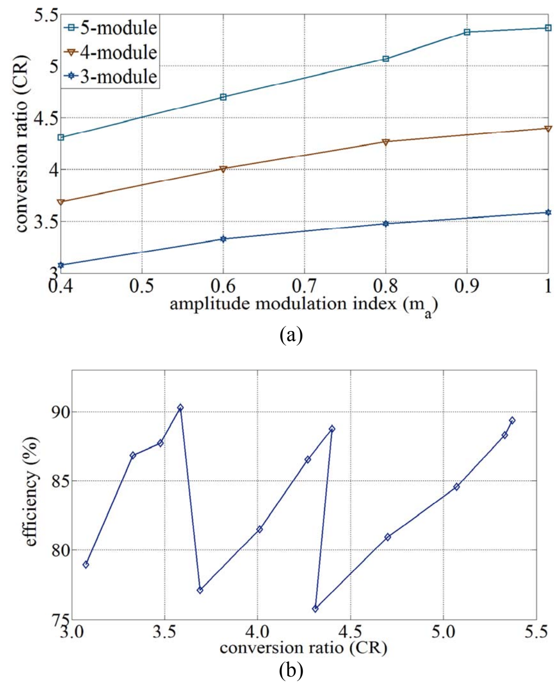

Fig. 6. Experimental results: (a) conversion ratio vs. amplitude modulation index (m_a), (b) conversion ratio vs. efficiency

switching transients. Each 4.7 μF capacitors were implemented by paralleling ten 0.47 μF ceramic capacitors

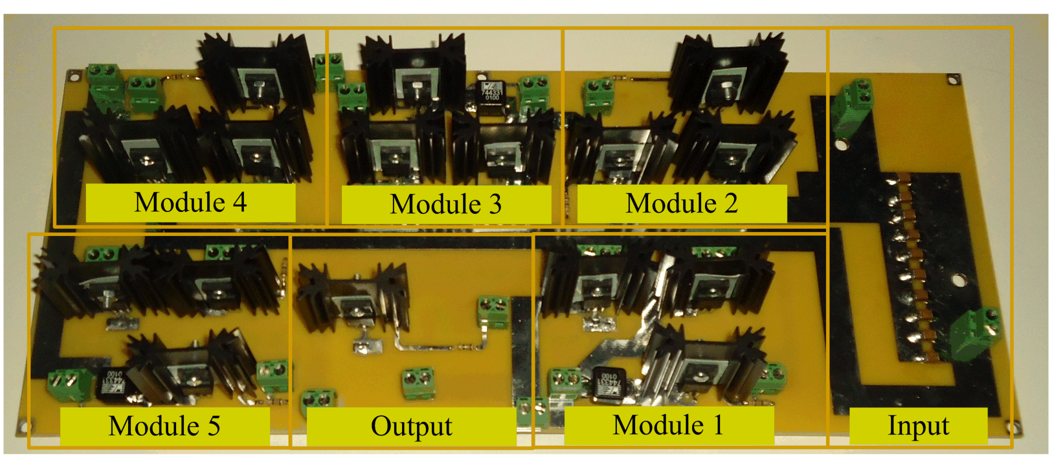

Fig. 7. Reconfigurable 5-module MMCCC prototype

(C4532X7T2W474K). This ceramic capacitors were chosen because of smaller size ((4.50mm x 3.20mm x 2.5mm) and low tolerance (±20 %). The 1 μH inductors were implemented using 1.0μH 21A SMD power-choke WE-HCC 1210 inductors. The saturation current rating of the inductor was 52 A. This inductor was chosen due to higher current carrying capability. The dimension of the inductor was 12.10mm x 11.40mm x 9.50mm. Therefore, inserting an inductor in each module of MMCCC will not increase the size of the converter to a significant amount. The frequency of the square wave and the triangular wave were set to 50 kHz and 10 kHz respectively. A 3711A DC electronic load was used as a resistive load. The resistance of the electronic load was set at 150 Ω. The input power was measured using a PM3000ACE-001 three phase power analyzer from Voltech Instruments Ltd.

The experimental results using 3, 4, and 5 modules are shown in Fig. 6. In Fig. 6(a), the CR is plotted vs. amplitude modulation index (m_a), and the efficiency vs. CR is plotted in Fig. 6(b). For a fixed number of active modules, the efficiency of the converter decreases with decreased CR. As the CR deviates from its ideal conversion ratio, the voltage ripple in each capacitor increases. This increased ripple in capacitor voltages increases the capacitor charging and discharging losses. However, inserting an inductor in each charging-discharging path minimizes the inrush current of that branch. Therefore, the peak of input current is also reduced. It reduces the peak current requirement of the input power source. The prototype is shown in Fig. 7. In Fig. 8, an oscilloscope capture of the gate signal and the output voltage are shown.

VI. CONCLUSIONS

A new switching scheme has been proposed in this paper demonstrating the capability to produce continuously variable conversion ratio (CR) using the MMCCC circuit. An additional inductor is added in each module of the MMCCC. This inductor decreases the input current ripple and ripple in the output voltage. The structure of MMCCC was utilized in order to insert the inductors without any need for snubber circuits. Continuous variation in conversion ratio was achieved using the proposed switching scheme. The concept is validated using both simulation and experimental results using a 5-module reconfigurable MMCCC prototype circuit.

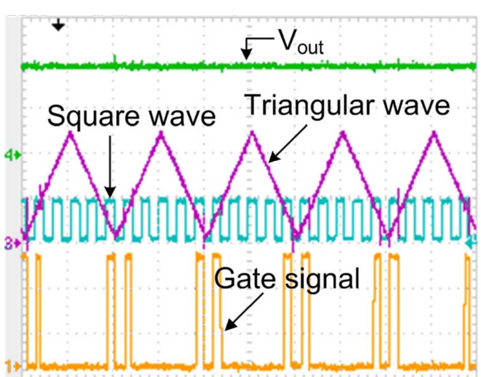

Fig. 8. Oscilloscope capture showing the switching pattern generation and output voltage wave shape

REFERENCES

[1] M. S. Makowski and D. Maksimovic, "Performance limits of switched-capacitor dc-dc converters," IEEE Power Electronics Specialists Conference, vol. 2, pp. 1215-1221, June 1995.

[2] Z. Pan, F. Zhang, and F. Z. Peng, "Power losses and efficiency analysis of multilevel dc-dc converters," IEEE Applied Power Electronics Conference, pp. 1393-1398, March 2005.

[3] Michael D. Seeman ,"A Design Methodology for Switched-Capacitor DC-DC Converters," Ph.D. Dissertation, University of California at Berkeley, May 2009, available at: URL: http://www.eecs.berkeley.edu/Pubs/TechRpts/2009/EECS-2009-78.pdf

[4] F. H. Khan, L. M. Tolbert, "A Multilevel Modular Capacitor Clamped DC_DC Converter," IEEE Industry Applications Society (IAS) Conference, Tampa, FL, Oct. 2006, pp. 966-973 (Award paper).

[5] F. H. Khan, L. M. Tolbert, "A Multilevel Modular Capacitor Clamped DC_DC Converter," IEEE Industry Applications Society (IAS) Conference, Tampa, FL, Oct. 2006, pp. 966-973 (Award paper).

[6] F. H. Khan, L. M. Tolbert, "Multiple Load-Source Integration in a Multilevel Modular Capacitor Clamped DC-DC Converter Featuring Fault Tolerant Capability," IEEE Applied Power Electronics Conference (APEC), Anaheim, CA, Feb. 2007, pp. 361-367.

[7] F. H. Khan, L. M. Tolbert, "Universal Multilevel DC-DC Converter with Variable Conversion Ratio, High Compactness Factor and Limited Isolation Feature," IEEE Applied Power Electronics Conference (APEC), Austin, TX, February 2008, pp. 17-23.

[8] F. H. Khan, L. M. Tolbert, "Generating Isolated Outputs in a Multilevel Modular Capacitor Clamped DC-DC Converter (MMCCC) for Hybrid Electric and Fuel Cell Vehicles," IEEE Power Electronics Specialists Conference (PESC), Rhodes, Greece, June 2008, pp. 967-973.

[9] F. H. Khan, L. M. Tolbert, "A Multilevel Modular Capacitor-Clamped DC-DC converter," IEEE Transactions on Industry Applications, vol. 43, no. 6, pp. 1628-1638, Nov. 2007.

[10] F. H. Khan, L. M. Tolbert, "Bi-directional Power Management and Fault Tolerant Feature in a 5 kW Multilevel DC-DC Converter with Modular Architecture," IET Power Electronics, vol. 2, no. 5, pp. 595-604, Sept. 2009.

[11] F. H. Khan, L. M. Tolbert, "Multiple Load-Source Integration in a Multilevel Modular Capacitor Clamped DC-DC Converter Featuring Fault Tolerant Capability," IEEE Transactions on Power Electronics, vol. 24, no. 1, pp. 14-24, Jan. 2009.

[12] F. H. Khan, L. M. Tolbert, "Startup and Dynamic Modeling of the MMCCC Converter," IEEE Transactons on Power Electronics, vol. 25, no. 2, pp. 519-531, Feb. 2010. M. S. Makowski "Voltage regulation in switched-capacitor converters—A problem revisited", Proc. 5th Eur. Space Power Conf., p.357 , 1998.

[13] D. Cao and F. Z. Peng, "Zero-current-switching multilevel modular switched-capacitor dc-dc converter," in *Energy Conversion Congress and Exposition, 2009. ECCE 2009. IEEE*, 2009, pp. 3516-3522.

[14] D. Cao and F. Z. Peng, "Zero current switching multi-level modular switched-capacitor dc-dc converter," IEEE transaction on industrial applications, vol. 46, no. 6, 2010, pp. 2536-2544.